Transient Suppression of Bacterial Populations Associated with Gut Health is Critical in Success of Exclusive Enteral Nutrition for Children with Crohn's Disease

Short Title: Microbial responses to Exclusive Enteral Nutrition

Joseph Runde[1,*], Iva Veseli[2], Emily C. Fogarty[3,4], Andrea R. Watson[3,4], Quentin Clayssen[4], Mahmoud Yosef[4], Alon Shaiber[4], Ritu Verma[5], Christopher Quince[6], Konstantinos Gerasimidis[7], David T. Rubin[4], A. Murat Eren[8,9,10,11*]

[1] Department of Pediatrics, Lurie Children's Hospital of Chicago, Chicago, IL 60611
[2] Biophysical Sciences Program, The University of Chicago, Chicago, IL 60637, USA
[3] Committee on Microbiology, The University of Chicago, Chicago, IL 60637, USA
[4] Department of Medicine, The University of Chicago, Chicago, IL 60637, USA
[5] Department of Pediatrics, The University of Chicago, Chicago, IL 60637, USA
[6] Organisms and Ecosystems, Earlham Institute, Norwich, Norwich, NR4 7UZ, United Kingdom
[7] School of Medicine, Dentistry & Nursing, University of Glasgow, Glasgow, G12 8QQ, Scotland
[8] Josephine Bay Paul Center, Marine Biological Laboratory, Woods Hole, MA 02543, USA
[9] Institute for Chemistry and Biology of the Marine Environment, University of Oldenburg, 26129, Oldenburg, Germany
[10] Alfred-Wegener-Institute for Marine and Polar Research, 27570 Bremerhaven, Germany
[11] Helmholtz Institute for Functional Marine Biodiversity, 26129 Oldenburg, Germany

* Correspondence: Joseph Runde, DO (jrunde@luriechildrens.org), A. Murat Eren, PhD (meren@hifmb.de).

Author Contributions:

JR and AME conceived the study. CQ and KG recruited patients, collected clinical and demographic data, and performed metagenomic sequencing. JR, IV, and AME analyzed data. EF, ARW, QC, and MY contributed to data analyses. IV, AS, and AME developed research tools. RV, DTR, and KG helped with clinical interpretations. JM, IV and AME wrote the paper with critical input from all authors.

Disclosures:

JR, IV, AW, EF, QC, MY, AS, RV, CQ, KG, and AME have no relevant disclosures. DTR has received grant support from Takeda; and has served as a consultant for Abbvie, Abgenomics, Allergan Inc., Arena Pharmaceuticals, Bellatrix Pharmaceuticals, Boehringer Ingelheim Ltd., Bristol-Myers Squibb, Celgene Corp/Syneos, Check-cap, Dizal Pharmaceuticals,

Abbreviations:

exclusive enteral nutrition (EEN)
genomic average nucleotide identity (gANI)
metagenome-assembled genome (MAG)
Pediatric Crohn's Disease Activity Index (PCDAI)

Transcript profiling:

https://doi.org/10.6084/m9.figshare.15108726.v1 gives reproducible access to the metagenome-assembled genomes generated in this study. Metagenomes are available via available in the European Nucleotide Archive (PRJEB7576).

Abstract

Background and Aims

Exclusive enteral nutrition (EEN) is a dietary intervention to induce clinical remission in children with active luminal Crohn's disease (CD). While changes in the gut microbial communities have been implicated in achieving this remission, a precise understanding of the role of microbial ecology in the restoration of gut homeostasis is lacking.

Methods

Here we reconstructed genomes from the gut metagenomes of twelve pediatric subjects who were sampled before, during, and after EEN. We then classified each microbial population into distinct 'phenotypes' or patterns of response based on changes in their relative abundances throughout the therapy on a per-individual basis.

Results

Our data show that children achieving clinical remission during therapy were enriched with microbial populations that were either suppressed or that demonstrated a transient bloom as a function of EEN. In contrast, this ecosystem level response was not observed in cases of EEN failure. Further analysis revealed that populations that were suppressed during EEN were significantly more prevalent in healthy children and adults across the globe compared with those that bloomed ephemerally during the therapy.

Conclusions

These observations taken together suggests that successful outcomes of EEN are marked by a temporary emergence of microbial populations that are rare in healthy individuals, and a concomitant reduction in microbes that are commonly associated with gut homeostasis. Our work is a first attempt to highlight individual-specific, complex environmental factors that influence microbial response in EEN. This model offers a novel, alternative viewpoint to traditional taxonomic strategies used to characterize associations with health and disease states.

Key Words: gut microbiome; genome-resolved metagenomics; microbial therapeutics

Introduction

Crohn's disease (CD), a type of inflammatory bowel disease (IBD), can affect any part of the gastrointestinal tract. Despite novel medical therapies and improved disease surveillance strategies, a medical cure does not exist and the risk of progression to surgery remains high.[1] The incidence of CD continues to rise in countries across the globe.[2] and data suggests that CD outcomes may be worse for those diagnosed as children.[3] The most effective medical therapies work through modification of the host immune system, which may result in sequelae of severe adverse effects and co-morbidities.[4-6] For this reason, diet-based therapies, which do not confer the same degree of risk, present an attractive alternative for patients and their families.[7]

One therapy, exclusive enteral nutrition (EEN), has proven efficacy for induction of clinical and endoscopic remission in pediatric subjects with CD. In fact, studies suggest that the rate of mucosal healing may be superior compared to other induction therapies such as systemic steroids.[8-12]

Additionally, the side effect profile of EEN is limited, and growth, an essential consideration in pediatric CD, is not compromised by this strategy.[13] The exact mechanism by which EEN works is not known. However, numerous studies have described dramatic shifts in taxonomic and functional compositions of gut microbial communities during EEN,[14-20] prompting researchers to suggest a role for the gut microbiome.[21] Nevertheless, the focus on microbial taxonomy has not yielded a particular set of taxa that is consistently associated with health or disease states. Furthermore, while some studies have identified organisms such as *Faecalibacterium prausnitzii* to have anti-inflammatory properties in CD,[22] other investigations of EEN in pediatric CD show that this organism decreases in abundance as a function of successful therapy.[16,23] These contrasting

observations reveal the need for deeper insights into the precise role of microbes in EEN-derived benefits.

A diverse gut microbial community is often associated with healthy gut homeostasis and host immunity,[24,25] while 'dysbiosis' is linked to states of active gut inflammation.[26,27] But this wisdom contrasts with successful applications of EEN, where remission in CD is associated with decreasing diversity during EEN therapy and its rebound once a normal diet is resumed.[14–17] To explain this phenomenon, some have postulated a superior "metabolic competence" allowing certain bacterial populations to succeed in dysbiosis based on their ability to utilize a rapidly-cycling carbohydrate input from the host.[28] When the diet is converted to a single, consistent carbohydrate this metabolic advantage is lost, creating an environment where other microbial residents may be more competitive.[28] This approach essentially shifts the focus from individual taxa to metabolic potential of microorganisms that survive EEN stress. If this is true, it is conceivable to expect that very closely related microbes with comparable metabolisms should respond similarly to EEN in different individuals. Given the interpersonal variation across human gut microbiomes, testing this hypothesis is difficult; however, using time-series data to characterize changes within each individual can shed light on microbiome dynamics as a response to therapy.

Here we apply genome-resolved metagenomics to characterize the response of microbial communities in the gut to EEN, without relying on taxonomy. From a previously established dataset of gut metagenomes from children with CD,[29] we reconstructed metagenome-assembled genomes (MAGs) from each individual independently and assigned each MAG a 'phenotype'

based on their responses to changing diet as indicated by the changes of the relative abundance of each MAG throughout the therapy in a given individual. Our findings demonstrate that positive EEN outcomes, such as clinical remission, are associated with a substantial ecosystem response to the change in diet. Our metagenomic read recruitment analyses using publicly available gut metagenomes showed that microbes that bloomed in children that responded to EEN were typically rare among healthy children and adults, while those that were suppressed in these patients were broadly detected in gut metagenomes of healthy individuals.

Materials and Methods

Shotgun metagenomes. We downloaded gut metagenomes using the accession numbers provided in the original manuscript by Quince et al.[29] Our dataset included 69 metagenomes 56 of which were from patients who were diagnosed with Crohn's disease (CD) and were sampled four to five times over the course of EEN therapy.[29] Characteristics of these children, including exposure to previous therapy, disease phenotype, and clinical response to EEN therapy are described in the original work.[29] We also used publicly available global gut metagenomes to benchmark our findings, accession IDs of which are listed in Supplementary Tables 1 and 2.

'Omics analyses. Whenever applicable, we automated and scaled our 'omics analyses using the bioinformatics workflows implemented by the program `anvi-run-workflow`[30] in anvi'o.[31,32] Anvi'o workflows implement numerous steps of bioinformatics tasks including short-read quality filtering, assembly, gene calling, functional annotation, hidden Markov model search, metagenomic read-recruitment and metagenomic binning. Workflows use Snakemake[33] and a tutorial is available at the URL http://merenlab.org/anvio-workflows/.

Metagenomic assembly and processing of contigs. We individually co-assembled the metagenomes from the same individual in our cohort using the IDBA-UD v1.1.3[34] with a minimum contig length of 1,000 bp. We then converted the resulting FASTA files to anvi'o contigs databases using the program `anvi-gen-contigs-database`, which (1) identified open reading frames in assembled sequences using Prodigal v2.6.3,[35] (2) predicted gene-level taxonomy using Centrifuge,[36] (3) annotated functions by aligning genes to the NCBI Clusters of Orthologous Groups (COG) database[37] with DIAMOND v0.9.31,[38] and (4) identified single-copy core genes by using HMMER

v3.2.1[39] to search for matches against a built-in collection of HMM profiles for bacteria and archaea in anvi'o. The average read recruitment rate of contigs back from the metagenomes from which they were assembled remained above 90% for each individual.

Read recruitment and binning. We used Bowtie2 v2.3.4.3[40] to recruit short reads from the set of metagenomes from each subject to the co-assembly of that subject's metagenomes, and samtools[41] to convert the SAM files into BAM files. We then used the programs `anvi-profile` to compute coverage and detection statistics, and `anvi-merge` to merge individual profiles, during which CONCOCT (Alneberg et. al., 2013) generated preliminary clusters of contigs based on their differential coverage and sequence composition. We then used the program `anvi-refine` to interactively and manually refine these preliminary clusters as described before.[42] We used the program `anvi-rename-bins` to determine bins that were over 70% complete as estimated by our bacterial single-copy core gene collection, assigned taxonomy to these 'metagenome-assembled genomes' (MAGs) using GTDB-Tk v0.3.2,[43] and used them for downstream analyses. To investigate the distribution of our genomes in publicly available data through metagenomic read recruitment, we used Bowtie2 v2.3.4.3[40] with default parameters and recovered coverage and detection statistics with anvi'o. We removed any bin from downstream analyses if it was less than 70% complete or more than 10% redundant after refinement based on 71 bacterial single-copy core genes.

Assignment of microbial population phenotypes. We assigned a 'phenotype' to each MAG from a single individual based on their distribution patterns across metagenomes from the same individual as revealed by read-recruitment. These phenotypes were: (1) Wilt: a decrease in

abundance by a factor of 10 from the pre-EEN metagenome to the post-EEN metagenome; (2) Suppressed: a decrease of abundance by a factor 10 in at least one metagenome during therapy that returns to pre-EEN abundance following therapy; (3) Ephemeral bloom: an increase in abundance by a factor of 10 seen in at least one time point during therapy that returns to pre-EEN abundance following therapy; (4) Sustained bloom: an increase of abundance following therapy by a factor of 10 compared with pre-EEN abundance estimates; (5) Stable: no changes of abundance of at least a factor of 10 at any time point throughout the time series; (6) Unclear: changes by a factor of 10 between values but does not fit into any described pattern above.

Calculating population relative abundances through read recruitment. We obtained percent abundance values for each MAG (in the patient it was binned from) by running `anvi-summarize` on each patient's co-assembly. We then normalized these values by dividing them by the maximum percent abundance value of the MAG in any sample from its source individual.

Mapping recovered MAGs in metagenomes of healthy children, mother-infant dyads and adults across countries. Shotgun metagenome sequences of healthy children from the original analysis (n=13)[29] publicly-available mother-infant dyads (n=392)[44] and healthy adults across six countries (n=939) were mapped against recovered MAGs to ascertain detection values. These values were then used to generate the box plots in Figure 3, and Wilcoxon signed-rank tests were used in each metagenome pool to determine the statistical difference between 'ephemeral' and 'suppressed' MAGs. For the healthy adult analysis 'ephemeral' and 'suppressed' MAGs from subjects with clinical remission were included (n=83), with three MAGs (two 'suppressed'; one

'ephemeral') from subject G10 due to our initial definition of clinical remission achieved after resuming a regular diet.

Dereplicating genomes. We dereplicated the 261 MAGs using the program `anvi-dereplicate-genomes` which used pyANI v0.2.9[45] to estimate the average nucleotide identity between each pair of MAGs across all individuals. A pair of MAGs was considered redundant if their average nucleotide identity (ANI) was over 97% with the alignment length covering at least 50% of the shorter genome. From each genome cluster that included more than one genome, we selected as a representative genome the one with the highest "completion minus redundancy" value based on the occurrence of bacterial single-copy core genes.

Genome-level analysis of microbial metabolism. We annotated each MAG with HMM hits to KOfam v94.0,[46] the database of KEGG Orthologs (KOs), using the program `anvi-run-kegg-kofams`, which uses HMMER[39] to match gene sequences to the KOfam HMM profiles. `anvi-run-kegg-kofams` discarded any KOfam hit that had a bit-score below noise cutoffs set by the KEGG. We then used the program `anvi-estimate-metabolism` to predict the metabolic capabilities of a given MAG. This program uses the KO annotations to compute the percent completion of each metabolic pathway in the KEGG MODULE database.[47] We used the scipy Python library for hierarchical clustering of MAGs according to their KEGG module completion scores.

Code and data availability. https://doi.org/10.6084/m9.figshare.15108726.v1 gives reproducible access to the metagenome-assembled genomes generated in this study. Metagenomes are available in the European Nucleotide Archive (PRJEB7576).

Results

Genome-resolved metagenomics yields 261 high-quality genomes from 12 children with Crohn's disease

In our previous study[29], twelve subjects were sampled four to five times before, during, and after EEN therapy. Baseline demographic and clinical information, along with disease activity indices were collected and are summarized in Table 1. To characterize the gut microbial ecology of each subject we reconstructed genomes from each individual independently (Figure 1) which enabled us to produce high-quality MAGS by applying differential coverage signals to minimize genome binning errors and risk of contamination.[48] Reconstructing genomes directly from gut metagenomes enables accurate tracking of microbial populations over time within a single individual[49] or across globally distributed human populations[50], and offers high-resolution descriptions of ecology beyond marker genes alone.[51]

Instead of assembling each metagenome in our dataset and reconstructing genomes independently from each time point, here we elected to co-assemble metagenomes that belonged to the same individual (Figure 1). A significant disadvantage of co-assemblies is the increased complexity of metagenomes due to remarkable inter-individual variability of the microbiome when data from multiple individuals are pooled. However, such risk is minimal for time-series data that cover relatively short time frames from a single individual. On the contrary, the pooled reads can lead to the recovery of more complete genomes for populations that are rare in every time point. Furthermore, the recovery of genomes from single-assembled metagenomes can yield genomes that are heavily contaminated due to lack of differential coverage signal.[48] Following the co-

assembly of each individual, we used sequence composition and differential coverage signal to cluster resulting contigs into a total of 589 metagenomic bins. We then removed any bins with less than 70% completion or greater than 10% redundancy, resulting in 261 high-quality genomes (Supplementary Table S1).

Overall, we recovered an average of 22 genomes from each subject that recruited more than 65% of the metagenomic reads (Supplementary Table S1). While our average genomes per subject was below the average of 31 genomes per sample in a recent global survey of gut metagenomes[52], our high read recruitment rate indicates that we were able to capture a high-quality version of the most abundant MAGs in each subject. There was not a statistically significant difference in the average number of genomes we were able to reconstruct between those children achieving clinical remission and those who did not (25 vs 18 genomes, respectively, p:0.1). The average number of metagenomic reads between samples from those achieving clinical remission did not significantly differ from one another (Wilcoxon, p-value: 0.5), which suggests that the depth of sequencing was relatively uniform among these samples (an average of ~8 million per sample and 40 million reads per individual via co-assembly used to reconstruct genomes). Although, there was a positive correlation (R^2: 0.5) between the number of genomes reconstructed per individual and the fraction of metagenomic reads they recruited (Supplementary Figure 3). The taxonomy of the MAGs we have reconstructed from these metagenomes matched to the previous taxonomic characterization of these data via 16S ribosomal RNA gene amplicons and shotgun metagenomic reads, with 16 of the 20 most common taxa being shared at the family level (Supplementary Table S1).

Clinical remission in EEN therapy is associated with a rise and fall in microbial population abundances

Our previous analysis of these data using amplicon sequences noted an overall reduction in diversity in microbial community composition in individuals who received EEN therapy.[29] Here, instead of describing general patterns emerging from the pooled data as a function of taxonomy, we characterized changes in relative abundance of microbial populations on a host-by-host basis, independent of their taxonomy. For this, we classified the microbial genomes reconstructed from each subject into 'phenotypes' based on changes in their relative abundance throughout EEN. We assumed that the change in relative abundance was significant between two time points if the proportion of reads recruited by the genome differed between the two samples by more than an order of magnitude (see methods for further detail).

While the relative abundance of some populations increased dramatically during EEN, the relative abundance of others decreased or did not change during therapy (Supplementary Table S1).. We divided these patterns of relative abundance into six 'phenotypes' (Figure 1): (1) 'suppressed' (population abundance is transiently decreased only during EEN therapy), (2) 'ephemeral' (population abundance is transiently increased only during EEN therapy, (3) 'wilt' (population is abundant only before therapy), (4) 'bloom' (population is abundant only after therapy), (5) 'stable' (the abundance of population does not fluctuate by more than an order of magnitude at any time point), and (6) 'unclear' (changes in population relative abundance throughout the study do not match to any of these patterns). For downstream analyses we primarily focused on 92 genomes, of which 40 belonged to the 'suppressed' and 52 belonged to the 'ephemeral' categories, since they represent populations that show the most marked response to EEN therapy (Figure 2).

We observed a significant difference in the proportion of 'ephemeral' and 'suppressed' populations between subjects who achieved clinical remission during EEN (defined as Pediatric Crohn's Disease Activity Index (PCDAI) <10) and those who did not (Wilcoxon nonparametric rank-sum test, p-value: 0.01) (Figure 2, Supplementary Table S1). Subject G21 was excluded from this analysis due to insufficient time-series data needed to assess phenotype response.

'Suppressed' and 'ephemeral' populations made up on average 45% of all microbial populations in individuals who showed clinical remission, and 10.1% of the populations recovered from individuals who did not (Figure 2, Supplementary Table S2).

Populations suppressed during EEN are common in healthy infants, children, and adults

Next, we sought to understand whether the populations that were suppressed or those that demonstrated an ephemeral bloom during EEN occurred more frequently in healthy infants, age-matched children, and healthy adults. First, we used metagenomic read recruitment to quantify the distribution of our genomes in publicly-available gut metagenomes from 98 healthy infants who were sampled within days of birth, at four months, and one year of life and 98 healthy women who gave birth to the infants[44]. This analysis revealed stark patterns of detection of our genomes based on phenotype assignment (Figure 3, Supplementary Table S2). While we were unable to detect most populations in our dataset in infant gut samples that were collected during the first few months of life, there was a marked increase in detection from samples that were collected from the same set of infants as they reached one year of life. (Figure 3, Supplementary Table S2). This

increase in detection among infant metagenomes was largely limited to 'suppressed' populations while 'ephemeral' populations remained poorly detected in all infant age groups (Wilcoxon nonparametric rank-sum test, p-value: 0.066). In the healthy mothers sampled in this dataset, differences in detection between suppressed and ephemeral populations were also significant (Wilcoxon nonparametric rank-sum test, p-value: 2.6e-07)

Next, we performed this analysis in 13 age-matched healthy children[29] where an even clearer difference in the detection of 'suppressed' and 'ephemeral' populations was appreciated (Wilcoxon nonparametric rank-sum test, p-value: 7.8e-08). (Figure 3, Supplementary Table S2).

Finding that microbial populations suppressed during EEN were common in these healthy datasets, we then performed a more comprehensive read recruitment analysis that included 939 additional adult gut metagenomes from six countries (Austria, Denmark, England, Italy, Spain, and the USA). This more robust analysis confirmed that populations that 'suppressed' during EEN were significantly more detected in every country studied compared to those that showed an 'ephemeral' phenotype during EEN (Wilcoxon nonparametric rank-sum test, p-value: 2.5e-0.6) (Figure 3, Supplementary Table S2).

'Identical' microbial populations in distinct individuals respond differently to EEN

Attempting to bypass the operational assumption of taxonomic assignment which postulates that populations that resolve to the same taxon are comparable across different individuals, or even different studies, we reconstructed genomes on an individual by individual basis. From this point,

we sought to investigate whether 'identical' MAGs recovered from unique children with CD behaved similarly in response to EEN.

Here, we used a de novo clustering strategy that relies solely on whole-genome sequence similarity to identify sequence discrete clusters within the collection of 261 genomes we have reconstructed from 12 individuals. Our clustering analysis using a similarity cutoff of 98% genomic average nucleotide identity (gANI) resulted in 123 clusters (Supplementary Table S3). The term 'identical' here does not imply 100% identity, rather it signifies that two populations have a gANI >= 98%; we note that this is more highly-resolved than taxonomic labels often assumed to confer sameness across individuals and studies.

Our results show that eight clusters contained six or more genomes, meaning that a genome recovered from one child on EEN in the study was more than 98% identical to a genome recovered in at least five other children. 56 clusters contained two or more genomes (recovered from two or more individuals independently) and 67 clusters contained a single genome (i.e., a genome reconstructed from an individual was not more than 98% identical to any other genome reconstructed from any of the individuals).

Each cluster described taxonomically and metabolically homogeneous genomes. Specifically, each genome that occurred in any of the 56 clusters that contained one or more genomes resolved to the same taxon name (Supplementary Table S3), and same hierarchical grouping of genomes based on KEGG metabolic modules (Supplementary Figure 1, Supplementary Table S3).

To our surprise, we found that clusters were rarely composed of genomes that were assigned to the same phenotype (Figure 4 highlights clusters with at least four genomes and Supplementary Table S3 includes full results in 'gANI clusters' tab). In fact, genome phenotypes within a cluster diverged to the extent that in several instances a population that was 'suppressed' during EEN therapy in one child was 'ephemeral' in another (Figure 4). In total, there were 47 instances where an 'identical' genome was recovered in at least two subjects and did not have a uniform phenotype, and only in 9 instances when all phenotypes within a cluster were the same (Supplementary Table S3). Overall, the dramatic difference in the phenotypic response of identical populations to EEN therapy suggests that taxonomically identical organisms should not be expected to respond similarly in different individuals.

Discussion

Our study offers a new ecological perspective on individual-based microbial responses to EEN therapy, a topic that has been traditionally investigated largely through cross-sectional taxonomic profiling of microbial communities. Examining changes in the relative abundance of microbial populations as a function of EEN in each patient, we observed dynamic, community-level shifts correlating with clinical remission in children with CD. Next, mapping to these populations with samples from healthy infants, children, and adults, we observed that 'suppressed' populations were significantly more detected than 'ephemeral' populations in healthy individuals. This conclusion is anchored in analysis from nearly 1,000 healthy adult individuals and this signal is detected as early as one year of life, perhaps, reflective of the transition to a more established gut constituency.[53] This observation gives greater understanding to the influence of EEN on the gut microbiota and raises important questions regarding our understanding of the determinants of successful microbial therapeutics in Crohn's disease and beyond.

A critical mechanism of EEN's efficacy is its ability to disrupt a microbial ecosystem, alter the inflammatory state of the gut microbiome and therefore temporarily change the mode of host-microbe interactions. This may be achieved by suppressing resident bacterial populations that are able to adapt and survive in the intestine of children with uncontrolled CD.

The transient emergence of microbes that are not primary members of healthy gut microbiomes and the temporary suppression of commonly-found microbes have implications on how to engineer new therapeutics for CD. While EEN has been primarily studied as a form of induction therapy, others have examined the long-term effects of partial enteral nutrition (around 50% of calories

consumed), both as adjunctive therapy in maintenance of remission[54,55] and as monotherapy.[56,57] Additionally, new dietary therapies mimicking the carbohydrate, protein and fat composition of traditional EEN have been proposed as effective for both induction and maintenance of remission in children with CD.[58]

Our findings suggest that EEN therapy likely functions less to restore homeostasis and acts more as an environmental stress to the gut community. As EEN temporarily pushes the gut composition away from its stable state, it may disrupt an injurious feedback loop associated with populations more fit to survive in the dysbiotic environment of CD. This concept of metabolic fitness is highlighted in other recent work from demonstrating that individuals with IBD are typically depleted of less metabolically competent populations.[59] Our results characterize these 'suppressed' populations as abundant across healthy individuals, tolerant of dysbiosis and effectively disrupted by the stress conferred via EEN.

As such, while EEN offers a highly effective means of induction therapy in pediatric CD, from a purely microbial ecology standpoint its use as a maintenance therapy is less consistent with our current understanding of gut homeostasis. Therefore, if EEN offers long-term benefit to gut health in pediatric CD as an uninterrupted therapy it is likely conveyed via another mechanism such as change in antigen profile, correction of intestinal permeability, or reduction of pro-inflammatory mediators.[60,61]

However, one means of potentially optimizing the critical microbial disruption highlighted in this study would be to use EEN as an intermittent therapy. This concept is under investigation,

examining the potential benefit of "cyclic" EEN as a form of maintenance therapy.[62] While further data is needed to substantiate this approach, conceptually it agrees with the findings presented here, maximizing the environment stress of EEN and any benefit derived from a temporary change in the gut microbiota.

While consideration of the taxa present before, during, and after EEN has been critical to our understanding of this important dietary intervention, attempting to catalog bacterial populations as commensal or pathogenic in the metagenomes of children undergoing a microbial therapy may be of limited utility. Here, we observe that a microbe's behavior is not uniform across subjects, and in some cases is paradoxical. In other words, learning about a genome/taxon in the global context does not necessarily predict its behavior in local contexts. In this case, the sum total of microbes with predicted "suppressed" or 'ephemeral' phenotypes before EEN therapy, given all the other members of a single gut community, may suggest that EEN will likely work to induce clinical remission in one individual and be less likely in another. This suggests that using existing gut microbiome data to help personalize therapy and predict outcomes may be more feasible than attempts to fundamentally and permanently change the community structure.

Recent efforts to better understand the probability of response to EEN have suggested that both taxonomic structure[21] and the metabolome may be predictive of success.[63,64] Our study offers an interesting association between the success of EEN and the enrichment of 'suppressed' and 'ephemeral' populations, which indicate a remarkable response to the changing environment within a single individual. Interestingly, we also observe that near-identical populations that are more than 98% identical at the genome level and that share the same species-level taxonomic classification, did not respond to the EEN consistently across individuals in our cohort. Our efforts

to investigate metabolic differences between such closely related genomes that resolved to the same gANI cluster of over 98% identity yet displayed different phenotypes across individuals did not yield additional insights (Supplementary Information). This may serve as evidence that the mechanisms driving microbial responses to change are far more complex than species-level taxonomy, and perhaps mediated by factors including genetic polymorphisms, variations at gene expression and/or metabolic output, and the presence, absence, or activity of extrachromosomal genetic elements such as plasmids or viruses.

As with other datasets studying the influence of EEN on the gut microbiome, interpretation of our results is limited by a small sample size, heterogeneous patient population, and the concomitant management strategies applied before and during the study period. We chose to focus on PCDAI as a marker for remission in this work, consistent with the approach taken in the initial publication of this dataset. While decline in the level of calprotectin from baseline may reflect better adherence to the diet[65] a recent meta-analysis of EEN studies suggests that PCDAI is also reliable marker of response.[66] Here we argue that our host-centric approach offers key insight into the behavior of microbial populations that are typically inaccessible through commonly used cross-sectional analyses in microbial ecology. However, we note that our phenotype assignment, which relies on posteriori analyses of data, offers little power to predict the response of a given taxon to EEN. We also acknowledge that similar analyses that rely on 'absolute abundance' of populations rather than their 'relative abundance' may yield different classes of phenotypes and might support different interpretations. Furthermore, a higher percentage of unmapped reads from metagenomes to the co-assembly in individuals without a significant response to EEN could result in lower MAG recovery. However, the diminished impact of therapy on the gut microbiota of these children may

also result in weaker differential coverage and a lower yield of MAGs. Even as sample size makes

statistical analysis less applicable for some results, our analysis benefits from time-series sample

collection, giving high resolution to the metagenomic-derived data and strength to the conclusions

reached.

Conclusions

This highly-resolved investigation of the gut community response in successful EEN therapy for pediatric CD reveals stereotypic phenotypes of bacterial populations under stress. We were able to validate these phenotypes by highlighting differences in distributions in those achieving clinical remission. Additionally, we demonstrate clear differences in global detection patterns of these phenotypes within healthy gut metagenomes. The 'omics strategies we have employed were unable to explain why 'identical' genomes do not have a uniform phenotypic response to EEN, underscoring the complexity of host-microbe interactions that call for host-centric, holobiont-approaches to drive much needed therapeutics for CD.

Acknowledgements:

References

1. Debruyn JCC, Soon IS, Hubbard J, Wrobel I, Panaccione R, Kaplan GG. Nationwide temporal trends in incidence of hospitalization and surgical intestinal resection in pediatric inflammatory bowel diseases in the United States from 1997 to 2009. *Inflamm Bowel Dis*. 2013;19(11):2423-2432.

2. Sýkora J, Pomahačová R, Kreslová M, Cvalínová D, Štych P, Schwarz J. Current global trends in the incidence of pediatric-onset inflammatory bowel disease. *World J Gastroenterol*. 2018;24(25):2741-2763.

3. Olén O, Askling J, Sachs MC, et al. Increased Mortality of Patients With Childhood-Onset Inflammatory Bowel Diseases, Compared With the General Population. *Gastroenterology*. 2019;156(3):614-622.

4. Kotlyar DS, Osterman MT, Diamond RH, et al. A systematic review of factors that contribute to hepatosplenic T-cell lymphoma in patients with inflammatory bowel disease. *Clin Gastroenterol Hepatol*. 2011;9(1):36-41.e1.

5. Ariyaratnam J, Subramanian V. Association between thiopurine use and nonmelanoma skin cancers in patients with inflammatory bowel disease: a meta-analysis. *Am J Gastroenterol*. 2014;109(2):163-169.

6. Long MD, Martin CF, Pipkin CA, Herfarth HH, Sandler RS, Kappelman MD. Risk of melanoma and nonmelanoma skin cancer among patients with inflammatory bowel disease. *Gastroenterology*. 2012;143(2):390-399.e1.

7. Svolos V, Gerasimidis K, Buchanan E, et al. Dietary treatment of Crohn's disease: perceptions of families with children treated by exclusive enteral nutrition, a questionnaire survey. *BMC Gastroenterology*. 2017;17(1). doi:10.1186/s12876-016-0564-7

8. Narula N, Dhillon A, Zhang D, Sherlock ME, Tondeur M, Zachos M. Enteral nutritional therapy for induction of remission in Crohn's disease. *Cochrane Database of Systematic Reviews*. Published online 2018. doi:10.1002/14651858.cd000542.pub3

9. Buchanan E, Gaunt WW, Cardigan T, Garrick V, McGrogan P, Russell RK. The use of exclusive enteral nutrition for induction of remission in children with Crohn's disease demonstrates that disease phenotype does not influence clinical remission. *Aliment Pharmacol Ther*. 2009;30(5):501-507.

10. Borrelli O, Cordischi L, Cirulli M, et al. Polymeric Diet Alone Versus Corticosteroids in the Treatment of Active Pediatric Crohn's Disease: A Randomized Controlled Open-Label Trial. *Clinical Gastroenterology and Hepatology*. 2006;4(6):744-753. doi:10.1016/j.cgh.2006.03.010

11. Grover Z, Burgess C, Muir R, Reilly C, Lewindon PJ. Early Mucosal Healing with Exclusive Enteral Nutrition is Associated with Improved Outcomes in Newly Diagnosed Children with Luminal Crohn's disease. *J Crohns Colitis*. 2016;10(10):1159-1164.

12. Pigneur B, Lepage P, Mondot S, et al. Mucosal Healing and Bacterial Composition in Response to Enteral Nutrition Vs Steroid-based Induction Therapy-A Randomised Prospective Clinical Trial in Children With Crohn's Disease. *J Crohns Colitis*. 2019;13(7):846-855.

13. Cohen-Dolev N, Sladek M, Hussey S, et al. Differences in outcomes over time with exclusive enteral nutrition compared with steroids in children with mild to moderate crohn's disease: results from the GROWTH CD Study. *J Crohns Colitis*. 2018;12(3):306-312.

14. Lionetti P, Callegari ML, Ferrari S, et al. Enteral nutrition and microflora in pediatric Crohn's disease. *JPEN J Parenter Enteral Nutr*. 2005;29(4 Suppl):S173-S175; discussion S175-S178, S184-S188.

15. Leach ST, Mitchell HM, Eng WR, Zhang L, Day AS. Sustained modulation of intestinal bacteria by exclusive enteral nutrition used to treat children with Crohn's disease. *Aliment Pharmacol Ther*. 2008;28(6):724-733.

16. Gerasimidis K, Bertz M, Hanske L, et al. Decline in presumptively protective gut bacterial species and metabolites are paradoxically associated with disease improvement in pediatric Crohn's disease during enteral nutrition. *Inflamm Bowel Dis*. 2014;20(5):861-871.

17. Dunn KA, Moore-Connors J, MacIntyre B, et al. Early Changes in Microbial Community Structure Are Associated with Sustained Remission After Nutritional Treatment of Pediatric Crohn's Disease. *Inflamm Bowel Dis*. 2016;22(12):2853-2862.

18. Kaakoush NO, Day AS, Leach ST, Lemberg DA, Nielsen S, Mitchell HM. Effect of exclusive enteral nutrition on the microbiota of children with newly diagnosed Crohn's disease. *Clin Transl Gastroenterol*. 2015;6:e71.

19. D'Argenio V, Precone V, Casaburi G, et al. An altered gut microbiome profile in a child affected by Crohn's disease normalized after nutritional therapy. *Am J Gastroenterol*. 2013;108(5):851-852.

20. Schwerd T, Frivolt K, Clavel T, et al. Exclusive enteral nutrition in active pediatric Crohn disease: Effects on intestinal microbiota and immune regulation. *J Allergy Clin Immunol*. 2016;138(2):592-596.

21. Jones CMA, Connors J, Dunn KA, et al. Bacterial Taxa and Functions Are Predictive of Sustained Remission Following Exclusive Enteral Nutrition in Pediatric Crohn's Disease. *Inflammatory Bowel Diseases*. 2020;26(7):1026-1037. doi:10.1093/ibd/izaa001

22. Sokol H, Pigneur B, Watterlot L, et al. Faecalibacterium prausnitzii is an anti-inflammatory commensal bacterium identified by gut microbiota analysis of Crohn disease patients. *Proc Natl Acad Sci U S A*. 2008;105(43):16731-16736.

23. Jia W, Whitehead RN, Griffiths L, et al. Is the abundance of Faecalibacterium prausnitzii relevant to Crohn's disease? *FEMS Microbiol Lett*. 2010;310(2):138-144.

24. Human Microbiome Project Consortium. Structure, function and diversity of the healthy human microbiome. *Nature*. 2012;486(7402):207-214.

25. Bäckhed F, Fraser CM, Ringel Y, et al. Defining a healthy human gut microbiome: current concepts, future directions, and clinical applications. *Cell Host Microbe*. 2012;12(5):611-622.

26. Imhann F, Vich Vila A, Bonder MJ, et al. Interplay of host genetics and gut microbiota underlying the onset and clinical presentation of inflammatory bowel disease. *Gut*. 2018;67(1):108-119.

27. Gevers D, Kugathasan S, Denson LA, et al. The treatment-naive microbiome in new-onset Crohn's disease. *Cell Host Microbe*. 2014;15(3):382-392.

28. Britto S, Kellermayer R. Carbohydrate Monotony as Protection and Treatment for Inflammatory Bowel Disease. *J Crohns Colitis*. 2019;13(7):942-948.

29. Quince C, Ijaz UZ, Loman N, et al. Extensive Modulation of the Fecal Metagenome in Children With Crohn's Disease During Exclusive Enteral Nutrition. *American Journal of Gastroenterology*. 2015;110(12):1718-1729. doi:10.1038/ajg.2015.357

30. Shaiber A, Willis AD, Delmont TO, et al. Functional and genetic markers of niche partitioning among enigmatic members of the human oral microbiome. *Genome Biol*. 2020;21(1):292.

31. Eren AM, Esen ÖC, Quince C, et al. Anvi'o: an advanced analysis and visualization platform for 'omics data. *PeerJ*. 2015;3:e1319.

32. Eren AM, Kiefl E, Shaiber A, et al. Community-led, integrated, reproducible multi-omics with anvi'o. *Nat Microbiol*. 2021;6(1):3-6.

33. Köster J, Rahmann S. Snakemake—a scalable bioinformatics workflow engine. *Bioinformatics*. 2012;28(19):2520-2522.

34. Peng Y, Leung HCM, Yiu SM, Chin FYL. IDBA-UD: a de novo assembler for single-cell and metagenomic sequencing data with highly uneven depth. *Bioinformatics*. 2012;28(11):1420-1428.

35. Hyatt D, Chen GL, Locascio PF, Land ML, Larimer FW, Hauser LJ. Prodigal: prokaryotic gene recognition and translation initiation site identification. *BMC Bioinformatics*. 2010;11:119.

36. Kim D, Song L, Breitwieser FP, Salzberg SL. Centrifuge: rapid and sensitive classification of metagenomic sequences. *Genome Res*. 2016;26(12):1721-1729.

37. Tatusov RL, Fedorova ND, Jackson JD, et al. The COG database: an updated version includes eukaryotes. *BMC Bioinformatics*. 2003;4:41.

38. Buchfink B, Xie C, Huson DH. Fast and sensitive protein alignment using DIAMOND. *Nat Methods*. 2015;12(1):59-60.

39. Eddy SR. Accelerated Profile HMM Searches. *PLoS Comput Biol*. 2011;7(10):e1002195.

40. Langmead B, Salzberg SL. Fast gapped-read alignment with Bowtie 2. *Nat Methods*. 2012;9(4):357-359.

41. Li H, Handsaker B, Wysoker A, et al. The Sequence Alignment/Map format and SAMtools. *Bioinformatics*. 2009;25(16):2078-2079.

42. Shaiber A, Willis AD, Delmont TO, et al. Functional and genetic markers of niche partitioning among enigmatic members of the human oral microbiome. *Genome Biol*. 2020;21(1):292.

43. Chaumeil PA, Mussig AJ, Hugenholtz P, Parks DH. GTDB-Tk: a toolkit to classify genomes with the Genome Taxonomy Database. *Bioinformatics*. Published online November 15, 2019. doi:10.1093/bioinformatics/btz848

44. Bäckhed F, Roswall J, Peng Y, et al. Dynamics and Stabilization of the Human Gut Microbiome during the First Year of Life. *Cell Host Microbe*. 2015;17(6):852.

45. Pritchard L, Glover RH, Humphris S, Elphinstone JG, Toth IK. Genomics and taxonomy in diagnostics for food security: soft-rotting enterobacterial plant pathogens. *Anal Methods*. 2016;8(1):12-24.

46. Aramaki T, Blanc-Mathieu R, Endo H, et al. KofamKOALA: KEGG Ortholog assignment based on profile HMM and adaptive score threshold. *Bioinformatics*. 2020;36(7):2251-2252.

47. Muto A, Kotera M, Tokimatsu T, Nakagawa Z, Goto S, Kanehisa M. Modular architecture of metabolic pathways revealed by conserved sequences of reactions. *J Chem Inf Model*. 2013;53(3):613-622.

48. Chen LX, Anantharaman K, Shaiber A, Eren AM, Banfield JF. Accurate and complete genomes from metagenomes. *Genome Res*. 2020;30(3):315-333.

49. Sharon I, Morowitz MJ, Thomas BC, Costello EK, Relman DA, Banfield JF. Time series community genomics analysis reveals rapid shifts in bacterial species, strains, and phage during infant gut colonization. *Genome Res*. 2013;23(1):111-120.

50. Lee STM, Kahn SA, Delmont TO, et al. Tracking microbial colonization in fecal microbiota transplantation experiments via genome-resolved metagenomics. *Microbiome*. 2017;5(1):50.

51. Quince C, Walker AW, Simpson JT, Loman NJ, Segata N. Shotgun metagenomics, from sampling to analysis. *Nat Biotechnol*. 2017;35(9):833-844.

52. Pasolli E, Asnicar F, Manara S, et al. Extensive Unexplored Human Microbiome Diversity Revealed by Over 150,000 Genomes from Metagenomes Spanning Age, Geography, and Lifestyle. *Cell*. 2019;176(3):649-662.e20.

53. Avershina E, Lundgård K, Sekelja M, et al. Transition from infant- to adult-like gut microbiota. *Environ Microbiol*. 2016;18(7):2226-2236.

54. Tanaka T, Takahama K, Kimura T, et al. Effect of concurrent elemental diet on infliximab treatment for Crohn's disease. *J Gastroenterol Hepatol*. 2006;21(7):1143-1149.

55. Yamamoto T, Nakahigashi M, Umegae S, Matsumoto K. Enteral nutrition for the maintenance of remission in Crohn's disease: a systematic review. *Eur J Gastroenterol Hepatol*. 2010;22(1):1-8.

56. Takagi S, Utsunomiya K, Kuriyama S, et al. Effectiveness of an "half elemental diet" as maintenance therapy for Crohn's disease: a randomized-controlled trial. *Alimentary Pharmacology and Therapeutics*. 2006;24(9):1333-1340. doi:10.1111/j.1365-2036.2006.03120.x

57. Davidson N, Rutsky J, Bricker JB, et al. 6 and 12-Month Outcomes After 90:10 Enteral Nutrition Induction Therapy in Pediatric Crohn's Disease. *J Pediatr Gastroenterol Nutr*. Published online May 27, 2022. doi:10.1097/MPG.0000000000003475

58. Svolos V, Hansen R, Nichols B, et al. Treatment of Active Crohn's Disease With an Ordinary Food-based Diet That Replicates Exclusive Enteral Nutrition. *Gastroenterology*. 2019;156(5):1354-1367.e6.

59. Watson AR, Füssel J, Veseli I, et al. Adaptive ecological processes and metabolic independence drive microbial colonization and resilience in the human gut. *bioRxiv*. Published online April 22, 2021:2021.03.02.433653. doi:10.1101/2021.03.02.433653

60. Johnson T, Macdonald S, Hill SM, Thomas A, Murphy MS. Treatment of active Crohn's disease in children using partial enteral nutrition with liquid formula: a randomised controlled trial. *Gut*. 2006;55(3):356-361.

61. Levine A, Sigall Boneh R, Wine E. Evolving role of diet in the pathogenesis and treatment of inflammatory bowel diseases. *Gut*. 2018;67(9):1726-1738.

62. Pigneur Arnaud B, Martinez-Vinson C, Bourmaud A, et al. OP15 Cyclic exclusive enteral nutrition to maintain longterm drug-free remission in Paediatric Crohn's Disease: The CD HOPE study of the GETAID pédiatrique. *J Crohns Colitis*. 2021;15(Supplement_1):S015-S015.

63. Diederen K, Li JV, Donachie GE, et al. Exclusive enteral nutrition mediates gut microbial and metabolic changes that are associated with remission in children with Crohn's disease. *Scientific Reports*. 2020;10(1). doi:10.1038/s41598-020-75306-z

64. Ghiboub M, Penny S, Verburgt CM, et al. Metabolome changes with diet-induced remission in pediatric Crohn's disease. *Gastroenterology*. Published online June 6, 2022. doi:10.1053/j.gastro.2022.05.050

65. Mckirdy S, Russell RK, Svolos V, et al. The Impact of Compliance During Exclusive Enteral Nutrition on Faecal Calprotectin in Children with Crohn's Disease. *J Pediatr Gastroenterol Nutr*. Published online February 22, 2022. doi:10.1097/MPG.0000000000003425

66. Sohouli MH, Fatahi S, Farahmand F, Alimadadi H, Seraj SS, Rohani P. Meta-analysis: efficacy of exclusive enteral nutrition as induction therapy on disease activity index, inflammation and growth factors in paediatric Crohn's disease. *Aliment Pharmacol Ther*. Published online June 24, 2022. doi:10.1111/apt.17109

Tables

Table 1: Demographic data, clinical information, and disease activity indices of all 12 pediatric subjects.

| Subject ID	Age (years)	Sex	Duration EEN (days)	Crohn's Phenotype	New Diagnosis	Calprotectin Start/End of EEN	PCDAI Start/End of EEN	Crohn's Medications	Antibiotic exposure
G01	8.4	Female	57	L3L4	Yes	1130/88	20/0	Lactulose (after EEN only)	No
G03	12.7	Female	56	L3L4	No	2076/39	27.5/5	5-ASA	No
G05	12.1	Male	56	L3L4	Yes	2262/2059	70/12.5	Azathioprine	No
G06	7.3	Male	56	L2	No	2102/718	37.5/5	Azathioprine	No
G08	14.6	Male	49	L3	Yes	2272/1686	57.5/10	Probiotic (after EEN only)	No
G09	12.3	Male	56	L3L4	No	2582/2461	25/15	Azathioprine, 5-ASA	No
G10	14.7	Female	40	L3L4	No	2188/2298	20/12.5	5-ASA, Methotrexate, folic acid	No
G11	12.9	Male	56	L2L4	Yes	2439/1724	37.5/5	Azathioprine, iron, 5-ASA (after EEN only)	No
G12	13.5	Male	Unknown*	L2L4	Yes	2390/2717	50/37.5	Azathioprine (after EEN)	No
G15	11.5	Male	54	L2L4	Yes	2089/77	30/7.5	None	No
G21	13.9	Female	65	L3	Yes	2474/1865	55/50	None	Yes**
G33	9.2	Male	54	L3L4	Yes	3114/106	42.5/0	Iron, 5-ASA (end of EEN only)	No

Figure Legends
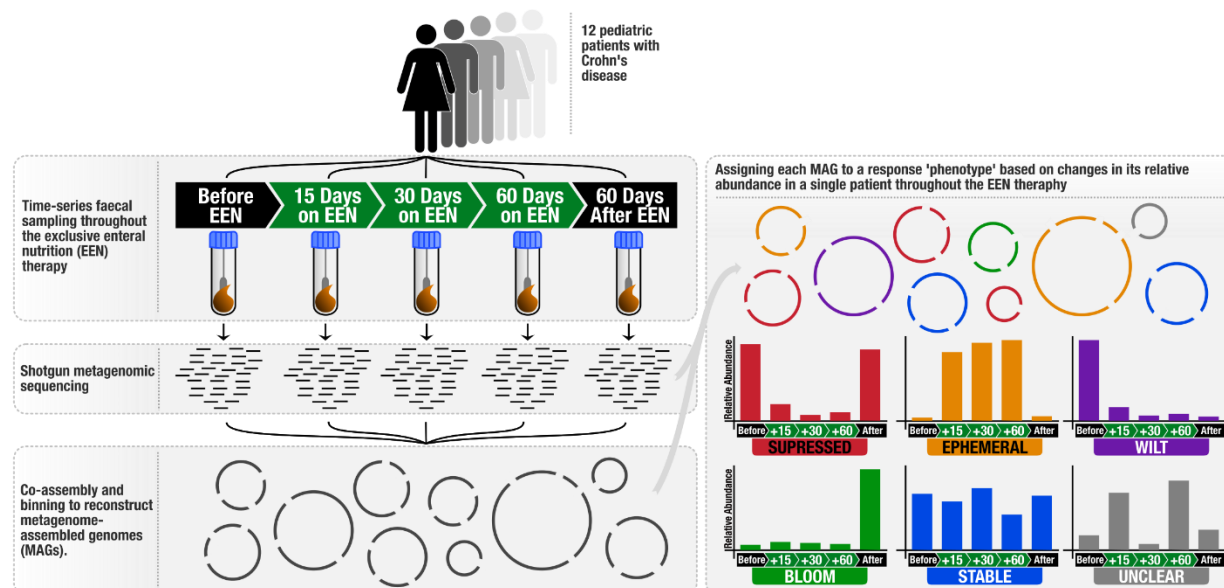
Figure 1. Overview of the sampling and analysis strategy, and the classification of genomes. Our metagenomic assembly and binning-based analysis of the shotgun sequencing of fecal metagenomes generated from 12 pediatric Crohn's disease patients who were sampled before, during, and after EEN therapy, resulted in microbial genomes reconstructed from each patient independently. We were then able to classify these genomes into distinct 'phenotypic' categories based on the changes of their relative abundance in a given individual over the course of EEN therapy.
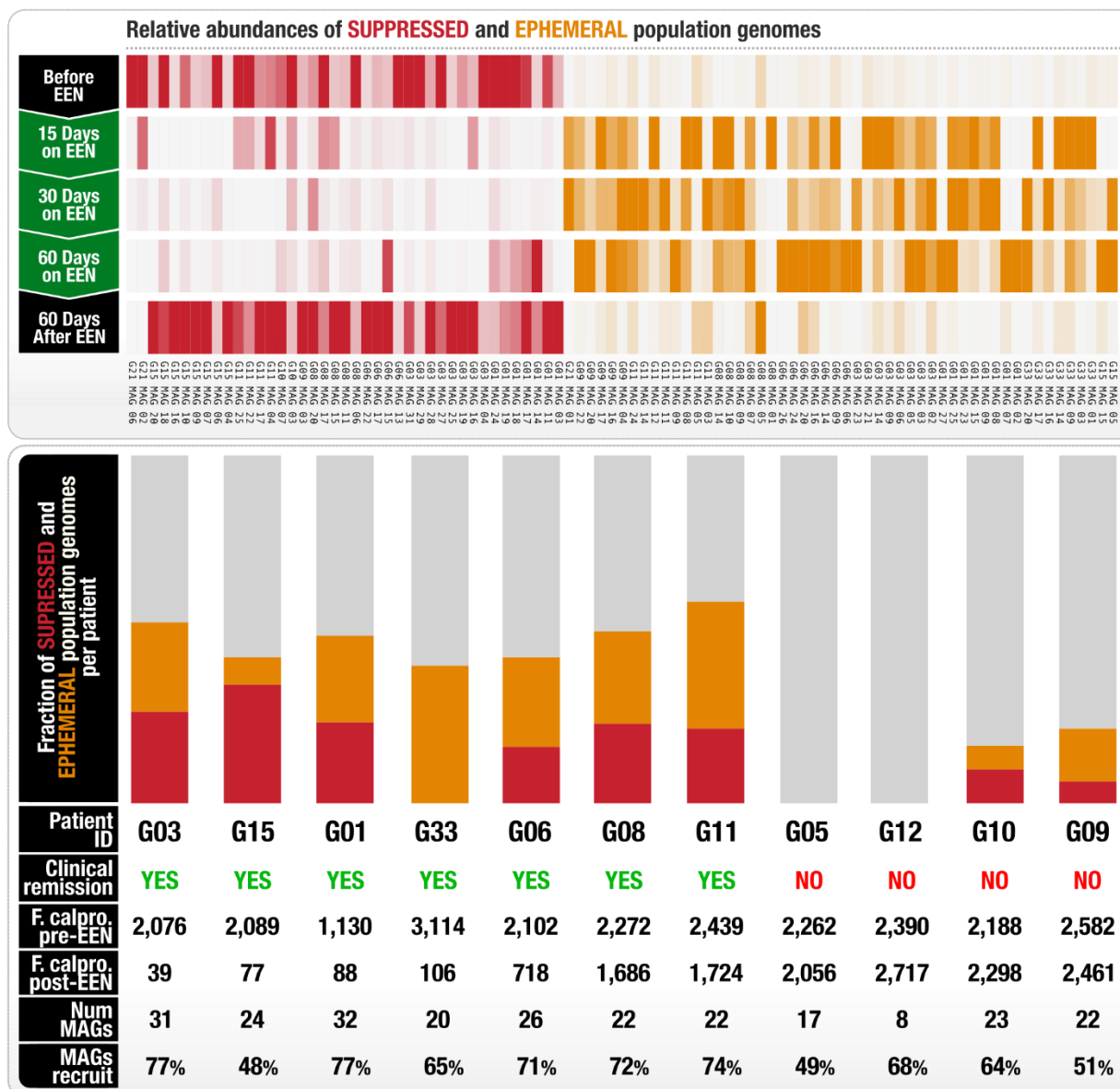
Figure 2. Genomes that showed 'suppressed' and 'Ephemeral' phenotypes. Each column in the top panel shows a single genome that is either classified as 'suppressed' (red) or 'ephemeral' (orange), where the intensity of colors indicate its relative abundance across the EEN therapy. The bottom panel shows for each individual, (1) the proportion of 'suppressed' and 'ephemeral' genomes recovered from each subject, where the gray color represents the proportion of genomes in a given patient that were classified into other phenotypes (i.e., neither 'suppressed' nor 'ephemeral'), (2) clinical response/remission status (based on PCDAI), (3) fecal calprotectin measurements before and after the EEN therapy, (4) the total number of genomes recovered, and (5) the percentage of metagenomic short reads MAGs recruit from the metagenomes from a given subject on average. (EEN: Exclusive enteral nutrition; F.Calpro: Fecal calprotectin; MAGs: Metagenome-assembled genomes). The percentage of reads via both assembly and MAG can be seen in Supplementary Figure 3.
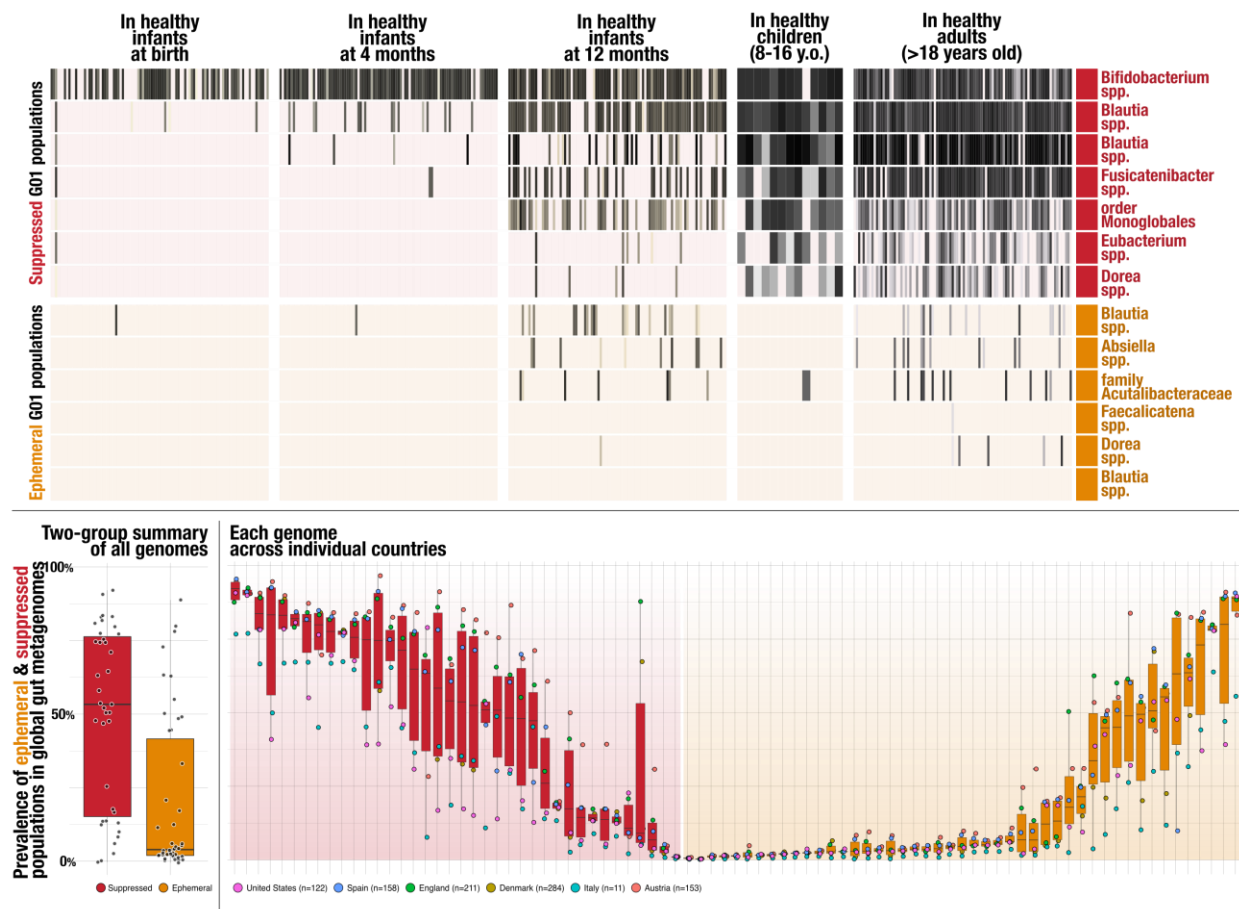
Figure 3. Distribution of 'suppressed' and 'ephemeral' populations in healthy individuals across age and geography. Each column in the heatmap in the top panel represents a metagenome from (1) healthy infants at birth, at 4 months, and 12 months, (2) healthy age-matching children to our cohort of pediatric patients, and (3) healthy adults. Data points in this heatmap show the detection of a given G01 'suppressed' (red) or 'ephemeral' (orange) genome in a given metagenome. The bottom panel shows the average detection values of all 'suppressed' (red) or 'ephemeral' (orange) genomes recovered from our patients in our study across 939 healthy adult gut metagenomes from six countries (box-plots on the left), and the detection values of each genome individually across the same set of metagenomes (box-plots on the right).
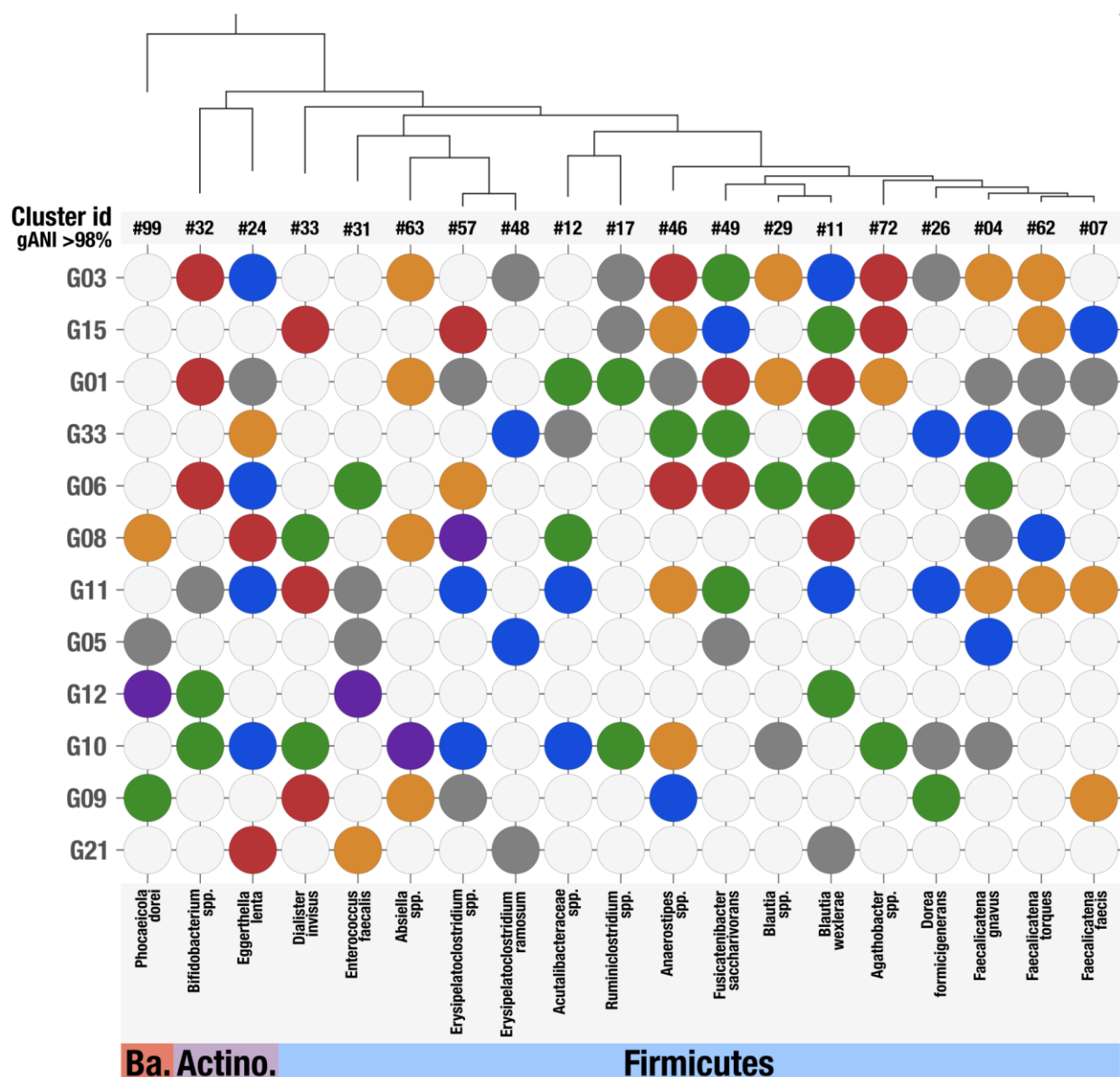
Figure 4. Phenotypes of genomes that are in the same 98% gANI cluster. Every column represents a cluster of genomes where every genome is >98% identical to others in the same cluster. The phylogenomic tree computed from ribosomal proteins of a representative genome from each cluster is shown at the top organizes genomes based on their evolutionary relatedness. Every row represents a patient, and colors indicate the class of a genome in a given individual as defined in Figure 1, where colors correspond to populations that were suppressed (red), ephemeral (orange), wilt (purple), bloom (green), stable (blue) and unclear (dark gray). For instance, if all genomes in a single column had the same color, this would have meant that every near-identical genome had a comparable change in their relative abundance as a function of the EEN therapy in a given individual. The best matching species-level taxon name for a given cluster according to GTDB is shown below, and colored bars represent bacterial phyla where Ba. stands for Bacteroidetes and Actino. Stands for Actinobacteria. Dots in light gray indicate those individuals who did not contribute a genome to a given cluster.

Supplementary Figure 1. Hierarchical clustering of 80 MAGs on the basis of their predicted metabolic capabilities demonstrates that MAGs from the same ANI-derived cluster are most similar in metabolic capacity. MAG names are color-coded by cluster membership.

Supplementary Figure 2. Hierarchical clustering of 1st and 3rd time point metagenomes shows stratification of responders and non-responders to EEN therapy. Samples are colored according to whether they belonged to a patient with CD patient that had clinically responded to EEN therapy (green), to a patient with CD that had no clinical response to EEN therapy (blue), or to a healthy control (black).

Supplementary Figure 3. Percent of reads mapped (y-axis) by both assembly (green) and metagenome-assembled genome (MAG) (orange) is shown according to subject with lighter shades demonstrating proportion of unmapped reads. Subjects are noted on the x-axis along the top of the figure with each subject divided into boxes. Within each subject box the metagenomes profiled are shown along the bottom (x-axis).

Tables Captions

Table 1: Demographic data, clinical information and disease activity indices of all 12 pediatric subjects. Age and sex of patient along with duration of EEN therapy and Crohn's phenotype based on Montreal classification is shown. Disease activity indices including fecal calprotectin measurements and PCDAI before and after EEN is reported. Medication exposure during therapy and use of antibiotics is also shown. PCDAI=pediatric Crohn's disease activity index; EEN: exclusive enteral nutrition; 5-ASA=5 aminosalicylate; *Minimum of 30 days; **On day 30 of therapy.

Supplementary Table S1. Description of co-assemblies, metagenomes, metagenome-assembled genomes and comparison of taxonomy between initial analysis and present study. Tab a) Co-assembly reads generated, recruited, contigs data and metagenomes-assembled. Tab b) Descriptive data of metagenome samples, clinical data and activity indices of corresponding subjects and accession ID. Tab c) Metagenome-assembled genomes phenotype assignment, contigs data, percent redundancy and completion, taxonomy and accession ID. Tab d) Comparison of the top 20 most abundant species and operational taxonomic units (OTUs) from initial analysis (two methods shotgun vs. 16s rRNA sequencing) and manual binning from study.

Supplementary Table S2. Detection, coverage and abundance of EEN Metagenome-assembled genomes (MAGs) in healthy children, mother-infant dyads and healthy adults. Tabs a-c) Metagenomes of healthy children from original study (n=13) with EEN MAG ID and phenotype ID in rows. Sample ID of healthy subjects in columns showing a) detection values; b) abundance values; c) Q2Q3 coverage values. Tabs d-f) Metagenomes of mother-infant dyads (n=98) with EEN MAG ID and phenotype ID in rows and mother-infant sample ID in columns. Columns are grouped with infant data at time point 0, 120 and 360 days followed by a corresponding maternal sample, repeating for all 98 dyads with d) detection values; e) abundance values; f) Q2Q3 coverage values. Tab g) Detection values of metagenomes of healthy adults across countries (n=939) with EEN MAG ID and phenotype ID in rows and healthy adults sample ID in columns (arranged by country). Only EEN MAGs of subjects with clinical response are included here. AST=Austria; DEN=Denmark; ENG=England; ITA=Italy; SPA=Spain; USA=United States of America. Tab h) Accession IDs and relevant metadata for public gut metagenomes used in this study (mother-infant dyads and healthy adults).

Supplementary Table S3. Description of gANI-derived clusters of EEN MAGs and metabolism estimation results for these MAGs. Tab a) gANI cluster membership of EEN MAGs in rows, with data including cluster size, MAG phenotype, and MAG taxonomy. White or gray shading is used to distinguish all genomes belonging to a given cluster. Tab b) Module completeness matrix output of `anvi-estimate-metabolism` for 80 MAGs from the 15 clusters with at least 4 genomes of differing phenotype. KEGG modules are in rows and EEN MAG IDs in columns, with each element in the matrix being a completeness score for a module within a MAG.

Supplementary Table S4. Data from metagenome-level metabolism estimation and enrichment analysis. Tab a) Metagenome samples that were used for metagenome-level metabolism estimation. Sample IDs are in rows. Sample group was assigned based on the subject's classification - healthy (H) for samples from healthy controls, responder (R) for samples from subjects who achieved clinical remission due to EEN, and non-responder (N) for samples from subjects who did not achieve clinical remission. Tab b) Module completeness matrix output of `anvi-estimate-metabolism` for these metagenomes. KEGG modules are in rows and sample IDs in columns, with each element in the matrix being a completeness score for a module within a metagenome. Metabolism completeness scores were estimated by treating the entire metagenome sample as one 'genome'; thus, these scores estimate the collective capabilities of all organisms in the metagenome sample rather than the metabolic capacities of individual populations. Tab c) Metabolism enrichment analysis output from `anvi-compute-functional-enrichment`, with KEGG modules in rows. Groups are defined as described in a).